

Influence of octupole deformation and orientation on the potential energy surface in the di-nuclear system model^{*}

WANG Nan(王楠)^{1,1)} ZHOU Shan-Gui(周善贵)^{2,3} ZHAO En-Guang(赵恩广)^{2,3} W. Scheid⁴

¹ College of Physics, Shenzhen University, Shenzhen 518060, China

² Institute of Theoretical Physics, Chinese Academy of Sciences, Beijing 100190, China

³ Center of Theoretical Nuclear Physics, National Laboratory of Heavy ion Accelerator, Lanzhou 730000, China

⁴ Institut für Theoretische Physik, Justus-Liebig-Universität, D-35392, Giessen, Germany

Abstract The nuclear and Coulomb potentials between deformed nuclei with octupole deformations and arbitrary orientations are evaluated numerically. The effects of the octupole deformation on the potential between nuclei and the potential energy surface (PES) used in the description of the production of super-heavy nuclei (SHN) by heavy-ion fusion reactions are investigated in the di-nuclear system model. It is found that the nuclear octupole deformation significantly changes the shape of the PES, which may influence the fusion probability of the SHN. Also, PESs in the tip-belly and belly-belly cases are investigated. Finally, the quasi-fission barriers in the tip-tip and belly-belly cases are evaluated. It is found that the quasi-fission barriers of the belly-belly case are generally larger than those of the tip-tip case.

Key words super-heavy nuclei, di-nuclear system model, potential energy surface

PACS 25.70.Jj, 24.10.-i, 25.60.Pj

1 Introduction

The activities of the synthesis of super-heavy nuclei (charge number $Z \geq 106$) are hotly maintained in both experimental and theoretical aspects. From the experimental aspect, the cold fusion reactions with Pb or Bi used as the target were performed to produce the super heavy nuclei with $Z=107-112$ [1]. In hot fusion reactions, the actinide nuclei were bombarded by the doubly magic nucleus ^{48}Ca and some heavier super-heavy nuclei were produced [2]. From the theoretical aspect, in order to reproduce and predict the evaporation residue cross sections and to understand the production mechanism of the super-heavy elements, several theoretical models were proposed, such as the di-nuclear system (DNS) model [3–8], the fluctuation-dissipation model [9, 10], the nuclear collectivization concept [11, 12] and the macroscopic dynamical model [13, 14].

In the DNS concept, the fusion process is considered as the evolution of a di-nuclear system by

means of the transfer of nucleons from the light nucleus to the heavy one. If one fragment is absorbed by the other one, a compound nucleus is formed. In Refs. [7, 8], the nucleon transfer process is described by solving the master equation numerically. It is found that the fusion probability of the compound nucleus is very sensitive to the potential energy surface in the mass asymmetry degree of freedom. Thus the study of the potential between two deformed nuclei and the potential energy surface is important for the theoretical study of the fusion probability and the fusion process. Also, from the results, we can estimate the magnitude of the deformation and orientation's contributions, which is important to understand the dynamical evolution of the nuclear shape and orientation, although the problem of the evolution is very difficult and has not been resolved satisfactorily. In Refs. [8, 15, 16], the effects of the quadrupole deformations on the potential energy surface (PES) and the fusion probabilities are investigated. It is shown that the quadrupole deformations affect the shape of

Received 18 May 2010

^{*} Supported by National Natural Science Foundation of China (10975100, 11011130216, 10979024, 10705014) and the financial support from DFG of Germany and Major State Basic Research Development Program of China (2007CB81500)

1) E-mail: wangnan@szu.edu.cn

©2010 Chinese Physical Society and the Institute of High Energy Physics of the Chinese Academy of Sciences and the Institute of Modern Physics of the Chinese Academy of Sciences and IOP Publishing Ltd

the PES and the height of the Businaro-Gallone (BG) point, and finally they influence strongly the fusion probabilities of the super-heavy nuclei (SHN). In some reactions leading to SHN, for example, $^{54}\text{Cr}+^{208}\text{Pb}$ and $^{64}\text{Ni}+^{208}\text{Pb}$, some nuclei with octupole deformations in the $Z \sim 88$ region may be involved in the nucleon transfer process [17–19]. Thus the PES and even the fusion probabilities could be affected by the octupole deformations and orientations. In this work, the nuclear and Coulomb potentials between two deformed nuclei with octupole deformations and arbitrary orientations are evaluated numerically with the double folding method. The effects of octupole deformations on the PES are evaluated. Also, the PES at some orientations and the quasi-fission barriers will be investigated.

The paper is organized as follows. In Section 2, the formalism for the nuclear potential, the Coulomb potential and the potential energy surface (i.e. the driving potential) is given. The results of the calculations and discussions about the interaction potentials and the potential energy surface for the super-heavy nuclei are presented in Section 3. Finally, a summary is given in Section 4.

2 Formalism for the potential energy surface in DNS and the potentials between deformed nuclei

In the DNS model, the potential energy surface, i.e., the driving potential, is very important because it provides information about the optimal projectile-target combination and excitation energy. The fusion probability is very sensitive to the structure of the potential energy surface [8]. For a di-nuclear system, the local excitation energy, which provides the excitation energy for the nucleon transfer, is defined as

$$\varepsilon^* = E - U(A_1, A_2) - \frac{(J - M)^2}{2\mathcal{J}_{\text{rel}}} - \frac{M^2}{2\mathcal{J}_{\text{int}}}, \quad (1)$$

where E is the energy of the composite system converted from the loss of the relative kinetic energy. $U(A_1, A_2)$ is the potential energy responsible for the nucleon transfer in the DNS model. J and \mathcal{J}_{rel} are the relative angular momentum and the relative moment of inertia of the DNS, respectively. M and \mathcal{J}_{int} denote the intrinsic spin due to the relative angular momentum dissipation and the corresponding moment of inertia, respectively. As a function of the mass asymmetry $\eta = \frac{A_1 - A_2}{A_1 + A_2}$, the PES in the DNS model is

defined as

$$U(A_1, A_2) = B(A_1) + B(A_2) - B^{\text{com}} + V_C(A_1, A_2) + V_N(A_1, A_2), \quad (2)$$

where $B(A_1)$, $B(A_2)$ and B^{com} are the binding energies for fragment 1, fragment 2 and the compound nucleus, respectively. $V_C(A_1, A_2)$ and $V_N(A_1, A_2)$ are the Coulomb potential and nuclear potential, respectively. The Coulomb potential can be calculated numerically as

$$V_C = \rho_1^0 \rho_2^0 \int \frac{d\vec{r}_1 d\vec{r}_2}{|\vec{r}_1 - \vec{r}_2 - \vec{R}|}, \quad (3)$$

where the integral runs over the two nuclei. \vec{R} is the vector between the two centers of the nuclei, as illustrated in Fig. 1. ρ_1^0 and ρ_2^0 are the charge densities of the two nuclei, respectively. The symmetry axes (\vec{S}_1 and \vec{S}_2) of the two deformed nuclei are assumed to be in the same plane. The surface of the deformed nucleus is expressed as $R(\alpha_i) = kR_{0i}[1 + \beta_2^i Y_{20}(\alpha_i) + \beta_3^i Y_{30}(\alpha_i) + \beta^i Y_{10}(\alpha_i)]$, where R_{0i} represents the radius of the spherical nucleus and k presents the conservation of the volume. The last term in the square brackets assures the constancy of the center of mass (C.M.). α_i is the angle between any vector \vec{R}_i and the symmetry axis \vec{S}_i , as shown in Fig. 1. The octupole deformation parameters can be taken as positive or negative values, which actually give the same nuclear shape. In this paper, we take positive octupole deformation parameters and the absolute octupole deformation values are taken from [17]. The direction from the center of the nucleus to the tip side is considered to be the positive direction. As shown in Fig. 1, the angles between the positive direction of symmetric axes and the z -axis for the two nuclei are γ_1 and γ_2 , respectively.

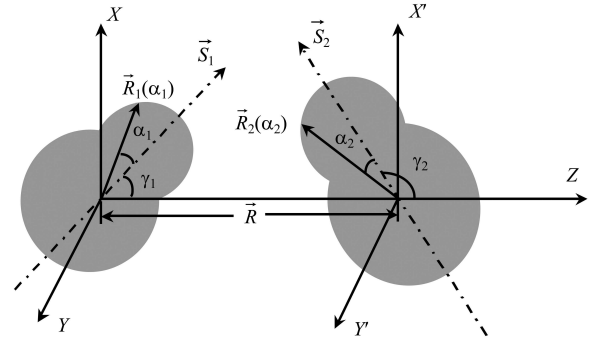


Fig. 1. Schematic presentation of the orientation of two deformed nuclei with axially symmetric quadrupole and octupole deformations.

For the nuclear potential, we adopt the Skyrme-type interaction without considering the momentum

and spin dependence. Under the sudden approximation, the nuclear potential between two nuclei can be calculated as [20]

$$V_N(R) = C_0 \left\{ \frac{F_{\text{in}} - F_{\text{ex}}}{\rho_{00}} \left[\int \rho_1^2(\vec{r}) \rho_2(\vec{r} - \vec{R}) d\vec{r} + \int \rho_1(\vec{r}) \rho_2^2(\vec{r} - \vec{R}) d\vec{r} \right] + F_{\text{ex}} \int \rho_1(\vec{r}) \rho_2(\vec{r} - \vec{R}) d\vec{r} \right\}, \quad (4)$$

with

$$F_{\text{in,ex}} = f_{\text{in,ex}} + f'_{\text{in,ex}} \frac{N_1 - Z_1}{A_1} \frac{N_2 - Z_2}{A_2}, \quad (5)$$

where $N_{1,2}$ and $Z_{1,2}$ are the neutron and proton numbers of the two nuclei, respectively. In this work, the parameters are taken as [15]: $C_0 = 300 \text{ MeV} \cdot \text{fm}^3$, $f_{\text{in}} = 0.09$, $f_{\text{ex}} = -2.59$, $f'_{\text{in}} = 0.42$, $f'_{\text{ex}} = 0.54$ and $\rho_{00} = 0.17 \text{ fm}^{-3}$. ρ_1 and ρ_2 are two-parameter Woods-Saxon density distributions for the two nuclei [15],

$$\rho_1(\vec{r}) = \frac{\rho_{00}}{1 + \exp\left(\frac{r - R_1(\alpha_1)}{a_{\rho 1}}\right)}, \quad (6)$$

$$\rho_2(\vec{r}) = \frac{\rho_{00}}{1 + \exp\left(\frac{|\vec{r} - \vec{R}| - R_2(\alpha_2)}{a_{\rho 2}}\right)}, \quad (7)$$

where $a_{\rho 1}$ and $a_{\rho 2}$ are the diffuseness parameters for the two nuclei, respectively.

3 Results and discussions

The nuclear+Coulomb potentials ($V_N + V_C$) at different nuclear orientations as a function of the C.M. separation r for the di-nuclear configurations $^{38}\text{S} + ^{224}\text{Th}$, which can form the compound nucleus $^{262}106$, and $^{60}\text{Fe} + ^{224}\text{Ra}$, which can form the compound nucleus $^{284}114$, are depicted in Figs. 2(a), (b), respectively. In Figs. 2(a), (b), we depict $0^\circ - 0^\circ$, $0^\circ - 90^\circ$ and $0^\circ - 180^\circ$ cases with solid, dotted and dashed lines, respectively. There are no orientation effects concerning the nucleus ^{38}S because it is spherical. The nucleus ^{224}Th is deformed with $\beta_2 = 0.164$ and $\beta_3 = 0.135$ [17]. The potentials between ^{38}S and ^{224}Th are shown in Fig. 2(a) for three orientations of the nucleus ^{224}Th , i.e., $\gamma_1 = 0^\circ$ and $\gamma_2 = 0^\circ$, 90° and 180° . Actually, $0^\circ - 0^\circ$ and $0^\circ - 180^\circ$ represent the “tip-bottom” and “tip-tip” cases, respectively. In Fig. 2(a), it can be seen that the barrier at the $0^\circ - 180^\circ$ (tip-tip) orientation is the lowest one, which is 10.48 MeV lower than that in the $0^\circ - 0^\circ$ (tip-bottom) case and 12.42 MeV lower than that in the $0^\circ - 90^\circ$

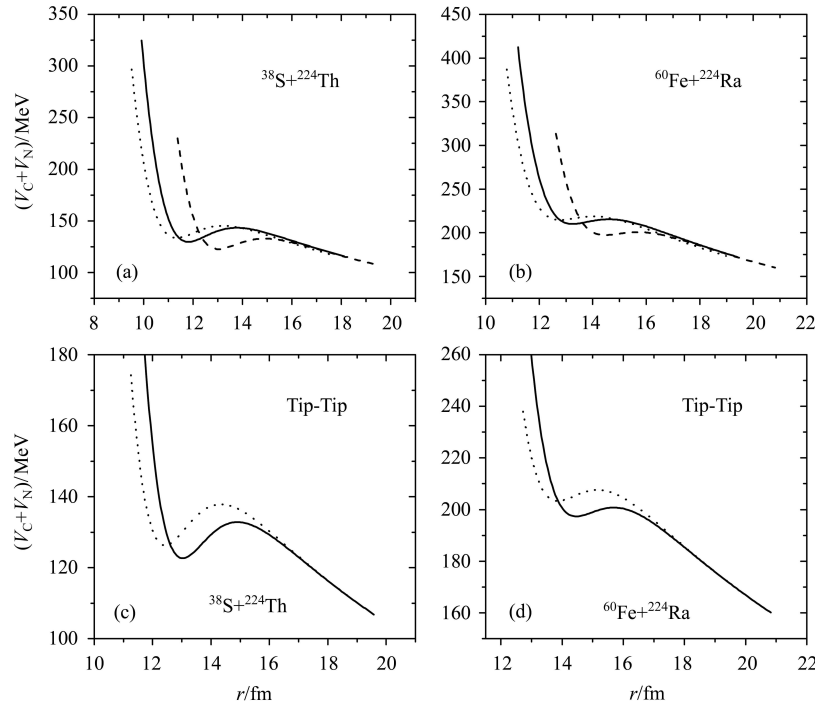


Fig. 2. Upper: Nuclear + Coulomb potentials for (a) $^{38}\text{S} + ^{224}\text{Th}$ and (b) $^{60}\text{Fe} + ^{224}\text{Ra}$ as functions of central distance between two nuclei at different nuclear orientations. For each reaction system, the orientation of the lighter nucleus is fixed at $\gamma_1 = 0^\circ$ and that of the heavier one γ_2 takes the value of 0° , 90° and 180° . Lower: Potentials of the reactions (c) $^{38}\text{S} + ^{224}\text{Th}$ and (d) $^{60}\text{Fe} + ^{224}\text{Ra}$ with the octupole deformation effects (solid curves) and without the octupole deformation effects (dotted curves) at the $0^\circ - 180^\circ$ (tip-tip) orientation.

(tip-belly) case. Thus, at a certain bombarding energy, a higher excitation energy can be obtained at the “tip-tip” orientation. It is also found that the 0° – 180° (tip-tip) orientation gives the largest C.M. separation for the minimum potential at the pocket position among the three orientations.

In Fig. 2, the nucleus ^{60}Fe is quadrupole deformed with $\beta_2 = 0.211$ and its octupole deformation is zero. Thus, the orientation angles 0° and 180° have the same physical meanings for ^{60}Fe because of its reflection symmetry. The quadrupole and octupole deformation parameters for the nucleus ^{224}Ra are $\beta_2 = 0.164$ and $\beta_3 = 0.131$ [17], respectively. The orientation angle for ^{60}Fe is set as $\gamma_1 = 0$, which implies that the symmetry axis of ^{60}Fe is parallel to the z axis. The potentials for three orientations of the nucleus ^{224}Ra are shown in Fig. 2(b). Similar situations as before can be found. The barrier at the 0° – 180° (tip-tip) orientation is the lowest one, and it is 14.68 MeV lower than that in the 0° – 0° (tip-bottom) case and 17.93 MeV lower than that in the 0° – 90° (tip-belly) case. It can be also seen that the 0° – 180° (tip-tip) orientation gives the largest C.M. separation for the minimum potential at the pocket position among the three orientations.

The nucleus-nucleus potentials of the reactions $^{38}\text{S}+^{224}\text{Th}$ and $^{60}\text{Fe}+^{224}\text{Ra}$ at the 0° – 180° (tip-tip) orientation with octupole deformation effects (solid curves) and without the octupole deformation effects (dotted curves) are shown in Fig. 2(c) and (d). In Fig. 2(c), the potential at the pocket position for the solid curve is 3.59 MeV lower than that for the dotted curve, which means that the octupole deformation affects the potential significantly. A similar situation can be found in Fig. 2(d) for the reaction $^{60}\text{Fe}+^{224}\text{Ra}$. At the 0° – 180° (tip-tip) orientation, the potential at the pocket position is decreased by 5.97 MeV due to the octupole deformation of ^{224}Ra .

The minimum potential at the pocket position V for $^{38}\text{S}+^{224}\text{Th}$ is given in Fig. 3(a) as a function of the orientation angle of ^{224}Th . Because the nucleus ^{224}Th is octupole deformed, the potential curve is asymmetric about the orientation angle $\gamma_2 = 90^\circ$. The maximum value is at about 100° and the minimum value at 180° . The minimum potential at the pocket position between ^{60}Fe and ^{224}Ra is presented in Fig. 3(b) as a function of the orientation angle γ_2 of ^{224}Ra with the orientation angle $\gamma_1 = 0$ for ^{60}Fe . Similar situations can be found in the two figures. The C.M. separations ΔR_C at the pocket positions between nuclei for $^{38}\text{S} + ^{224}\text{Th}$ and $^{60}\text{Fe} + ^{224}\text{Ra}$ are shown in Fig. 3(c) with a

solid circle line and an open circle line, respectively. From Fig. 3(c), it can be seen that the C.M. separations fluctuate with the angle γ_2 . The maximum potential can be obtained at about the minimum of ΔR_C while the minimum potential can be obtained at the maximum of ΔR_C .

The potential energy surfaces for the heavy-ion reactions $^{54}\text{Cr}+^{208}\text{Pb} \rightarrow ^{262}106$, $^{64}\text{Ni}+^{208}\text{Pb} \rightarrow ^{272}110$, $^{76}\text{Ge}+^{208}\text{Pb} \rightarrow ^{284}114$, and $^{92}\text{Kr}+^{208}\text{Pb} \rightarrow ^{300}118$ as a function of mass asymmetry η are depicted in Fig. 4. Only the part $-1 < \eta < 0$ of the PES is shown because of the symmetric structure of PES. The solid circle and open circle lines represent the results for the tip-tip and tip-bottom orientations, respectively. The PES where the nuclear octupole deformation is neglected is also given in Fig. 4 (the triangle line) for comparison. The arrow in the figure shows the incident channels η_i . It can be seen that the shape of the potential energy surface is modified because of the nuclear octupole deformation. For the channel $^{76}\text{Ge}+^{208}\text{Pb} \rightarrow ^{284}114$, in the region between $\eta \sim -0.6$ and $\eta \sim -0.5$, the solid circle line is 6–8 MeV lower than the triangle line, which means that the potential energy of the tip-tip orientation decreases because of the octupole deformation. For example, at $\eta = -0.5352$, the potential energies with and without considering the octupole deformation in the tip-tip case are found to be -8.59 MeV and -1.20 MeV, respectively. The difference is 7.39 MeV. Then a pocket on the left side (larger value of $|\eta|$) of the incident channel can be formed, which may store some probabilities and to some extent prevent the di-nuclear system from moving rapidly to the symmetric direction in η . In this sense, fusion will be enhanced. It can also be seen that the open circle lines (potential energies at the tip-bottom orientation) are higher than the triangle lines (without the octupole deformation effects). In this situation, fusion may be hindered because a high barrier prevents the formation of more asymmetric di-nuclear systems by the transfer of nucleon(s). In Fig. 4(c), near the mass symmetry configurations $\eta \sim 0$, it can be seen that the octupole deformations also decrease the potential energies in the tip-tip case. However, this region is far from the incident channel and near the mass symmetric configuration where the di-nuclear systems are very likely to separate by quasi-fission. Thus, the change in the shape of PES in this region has less influence than that in the region on the left side of the incident channel. In the other three figures, similar situations can be found.

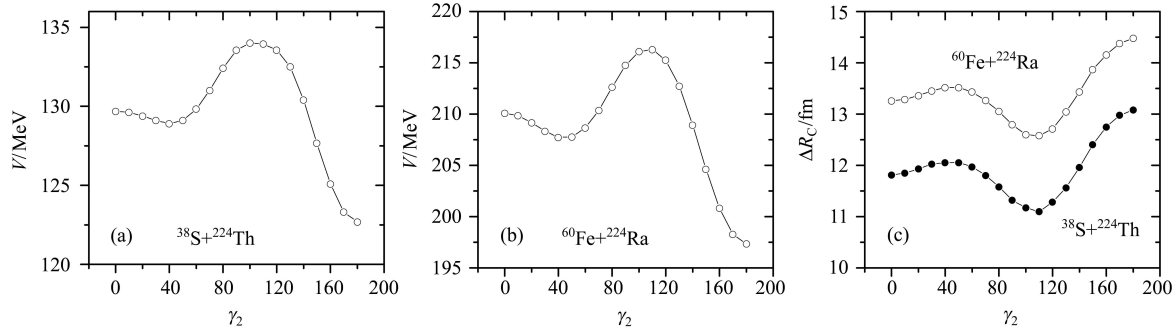


Fig. 3. Left and middle: The minimum potential at the pocket position as a function of the orientation angle γ_2 for (a) $^{38}\text{S}+^{224}\text{Th}$ and (b) $^{60}\text{Fe}+^{224}\text{Ra}$. Right: The C.M. separations between nuclei for $^{38}\text{S}+^{224}\text{Th}$ (solid circle line) and $^{60}\text{Fe}+^{224}\text{Ra}$ (open circle line), respectively.

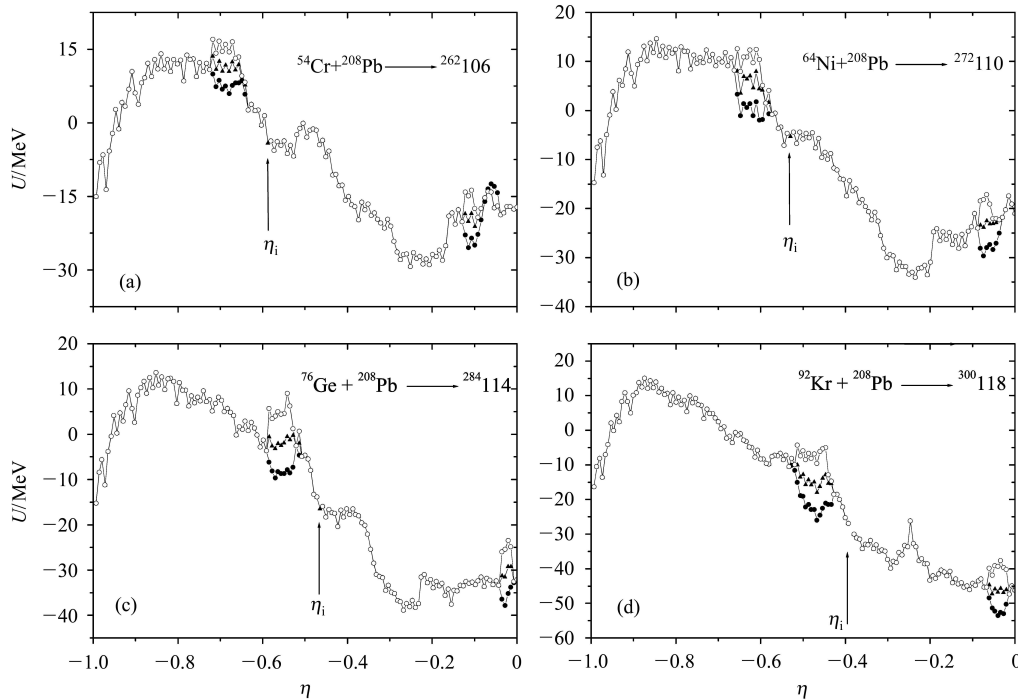


Fig. 4. Potential energy surfaces for (a) $^{54}\text{Cr}+^{208}\text{Pb} \rightarrow ^{262}106$, (b) $^{64}\text{Ni}+^{208}\text{Pb} \rightarrow ^{272}110$, (c) $^{76}\text{Ge}+^{208}\text{Pb} \rightarrow ^{284}114$ and (d) $^{92}\text{Kr}+^{208}\text{Pb} \rightarrow ^{300}118$. The solid circle and open circle lines represent the results for the tip-tip and tip-bottom orientations, respectively. The driving potential obtained from the calculation with the nuclear octupole deformation neglected is also given (the triangle line) for comparison.

The potential energy surfaces for $^{76}\text{Ge}+^{208}\text{Pb} \rightarrow ^{284}114$ in the tip-belly and belly-belly cases are depicted in Figs. 5(a) and (b), respectively. It can be seen that the structure of the PES at the two orientations is quite different from that of the tip-tip case. For example, the mass asymmetry of the BG point in the belly-belly case ($\eta_{\text{BG}} = -0.7535$) is closer to the incident channel than that in the tip-tip case ($\eta_{\text{BG}} = -0.8521$). The height of the BG point in the belly-belly case ($U_{\text{BG}} = 21.63$ MeV) is higher than that in the tip-tip case ($U_{\text{BG}} = 13.59$ MeV). The inner-fusion barrier (the barrier between the incident channel and

the BG point) for tip-tip, tip-belly and belly-belly cases is 30.05 MeV, 38.09 MeV and 30.92 MeV, respectively. On the right hand side of the incident channel, a barrier B_S can be found which prevents the system from moving to symmetric configurations. The barrier B_S in the tip-tip, tip-belly and belly-belly cases is, respectively, 0.47 MeV, 10.79 MeV and 18.99 MeV. The results imply that it is easy for a di-nuclear system in the tip-tip case to move to mass symmetry, which will finally lead to quasi-fission. However, it is difficult for the system in the belly-belly case to move to symmetric configurations.

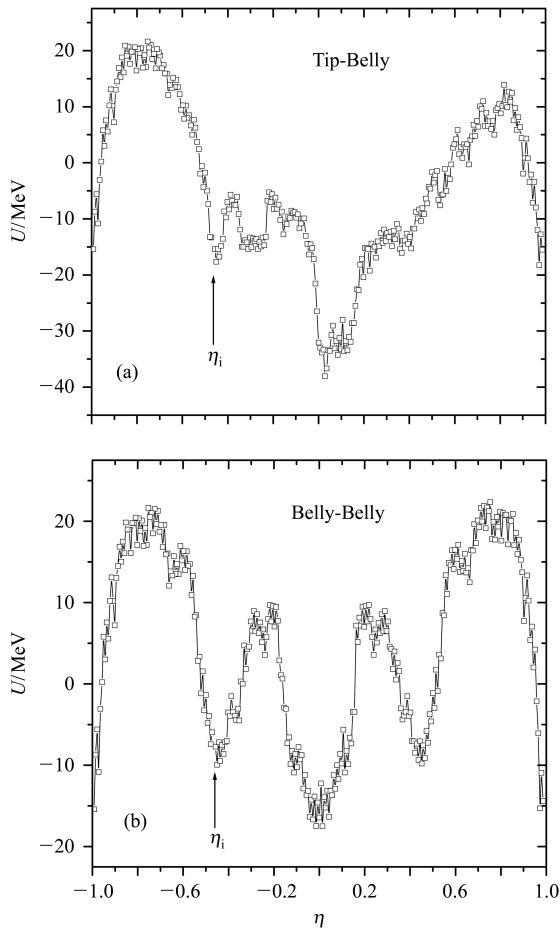


Fig. 5. Potential energy surfaces at (a) tip-belly and (b) belly-belly cases for ${}^{76}\text{Ge}+{}^{208}\text{Pb} \rightarrow {}^{284}114$.

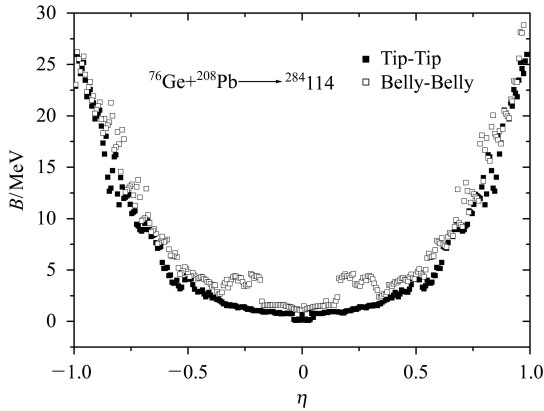


Fig. 6. The quasi-fission barriers for ${}^{76}\text{Ge}+{}^{208}\text{Pb} \rightarrow {}^{284}114$ as functions of the mass asymmetry η at the tip-tip and belly-belly orientations.

The quasi-fission barriers for ${}^{76}\text{Ge}+{}^{208}\text{Pb} \rightarrow {}^{284}114$ as a function of the mass asymmetry η are shown in Fig. 6 for the tip-tip and belly-belly orientations with solid and open dots, respectively. Generally speaking, the quasi-fission barrier increases with

an increasing absolute value for the mass asymmetry $|\eta|$. Thus, it is easier for a more symmetric system to separate by means of quasi-fission. In Fig. 6, we can find that the quasi-fission barriers in the belly-belly case are generally larger than those in the tip-tip case. For example, for the incident channel, the quasi-fission barrier in the belly-belly case is 1.19 MeV higher than that in the tip-tip case. In our calculations, we also find that in the tip-tip case, the quasi-fission barriers with the octupole deformations considered are about 1 MeV lower than those where the octupole deformations are neglected. For example, at $\eta = -0.5704$, the difference between the two cases is 0.943 MeV. Therefore, the contribution of the octupole deformation to the quasi-fission barrier should not be neglected.

4 Summary

The nuclear and Coulomb potentials between octupole-deformed nuclei with arbitrary orientations are evaluated numerically. The effects of the octupole deformations on the potential between nuclei and the potential energy surface (PES) used in the description of heavy-ion fusion reactions are investigated. It is found that the nuclear octupole deformations decrease the potential between octupole deformed nuclei and change the shape of the potential energy surface for producing super-heavy nuclei (SHN) significantly, which influences the fusion probability for the SHN. The PES in the tip-belly and belly-belly cases are also evaluated. We found that the quasi-fission barriers in the belly-belly case are larger than those in the tip-tip case and the octupole deformations decrease the quasi-fission barriers by about 1 MeV in the tip-tip case for some di-nuclear systems. This may enhance the quasi-fission process.

In future work, the fusion probability, the deformation and orientation effects should be investigated further. Actually, the dynamical evolution of the deformation and orientation is very difficult to treat satisfactorily. Our investigation may give an estimation of the magnitude of the effects of deformation and orientation to some extent and give a hint for further investigation.

The authors (Wang N, Zhou S G and Zhao E G) acknowledge the warm hospitality of the Institut für Theoretische Physik, Universität Giessen, Germany. They are also grateful to Prof. R. V. Jolos and Prof. Li J Q for valuable discussions.

References

- 1 Hofmann S, Münzenberg G. *Rev. Mod. Phys.*, 2000, **72**: 733; Hofmann S. *Rep. Prog. Phys.*, 1998, **61**: 639
- 2 Oganessian Yu. *Nucl. Part. Phys.*, 2007, **34**: 165, Hofmann S, Ackermann D, Antalic S et al. *Eur. Phys. J A*, 2007, **32**: 251
- 3 Volkov V V. *Izv. Akad. Nauk SSSR, Ser. Fiz.*, 1986, **50**: 1879
- 4 Antonenko N V, Cherepanov E A, Nasirov A K, Permjakov V P, Volkov V V. *Phys. Lett. B*, 1993, **319**: 425; *Phys. Rev. C*, 1995, **51**: 2635
- 5 Adamian G G, Antonenko N V, Scheid W, Volkov V V. *Nucl. Phys. A*, 1997, **627**: 361
- 6 Adamian G G, Antonenko N V, Scheid W. *Nucl. Phys. A*, 2000, **678**: 24–38
- 7 LI W F, WANG N, LI J F et al. *Europhys. Lett.*, 2003, **64**: 750
- 8 LI W F, WANG N, JIA J et al. *J. Phys. G*, 2006, **32**: 1143
- 9 Abe Y, Bouriquet B. *Nucl. Phys. A*, 2003, **722**: 241; 2004, **733**: 321(E)
- 10 SHEN C W, Kosenko G, Abe Y. *Phys. Rev. C*, 2002, **66**: 061602
- 11 Zagrebaev V I. *Phys. Rev. C*, 2001, **64**: 034606
- 12 Zagrebaev V I. *Nucl. Phys. A*, 2004, **734**: 164
- 13 Swiatecki W J. *Phys. Scr.*, 1981, **24**: 113
- 14 Blocki J P, Feldmeier H, Swiatecki W J. *Nucl. Phys. A*, 1986, **459**: 145
- 15 LI Q, ZUO W, LI W et al. *Eur. Phys. J. A*, 2005, **24**: 223
- 16 WANG N, LI J Q, ZHAO E G. *Phys. Rev. C*, 2008, **78**: 054607
- 17 Möller P, Nix J R, Myers W D, Swiatecki W J. *At. Data Nucl. Data Tables*, 1995, **59**: 185
- 18 Nazarewicz W, Olanders P, Ragnarsson I et al. *Nucl. Phys. A*, 1984, **429**: 269
- 19 Sobiczewski A, Muntian I, Patyk Z. *Phys. Rev. C*, 2001, **63**: 034306
- 20 Adamian G G, Antonenko N V, Jolos R V, Ivanova S P, Melnikova O I. *Int. J. Mod. Phys. E*, 1996, **5**: 191